JOURNAL OF MATERIALS SCIENCE 16 (1981) 2233–2245

The strength of hybrid glass/carbon fibre composites

Part 1 *Failure strain enhancement and failure mode*

P. W. MANDERS, M. G. BADER
Department of Metallurgy and Materials Technology, University of Surrey, Guildford, UK

The tensile mechanical properties of hybrid composites fabricated from glass and carbon fibres in an epoxy matrix have been evaluated over a range of glass:carbon ratios and states of dispersion of the two phases. The failure strain of the carbon phase increased as the relative proportion of carbon fibre was decreased, and as the carbon fibre was more finely dispersed. This behaviour is commonly termed the "hybrid effect", and failure strain enhancement of up to 50% has been measured. Only part of the effect may be attributed to internal compressive strains induced in the carbon phase by differential thermal contraction as the composite is cooled from its cure temperature. The laminae or ligaments of carbon fibre dispersed in the glass fibre phase show a multiple failure mode, and when the constitution is favourable catastrophic failure does not occur until a considerable number of ligament fractures have accumulated. Failure is thus progressive, and the material is effectively "tougher" than equivalent all-carbon fibre composites.

Nomenclature

CFP	carbon fibre reinforced phase.
GFP	glass fibre reinforced phase.
AL	alternating laminate series of specimens.
DT	divided-tow series of specimens.
ST	spread-tow series of specimens.
G	E-glass fibre.
HMS	high-modulus surface-treated carbon fibre.
HTS	high-tensile surface-treated carbon fibre.
AE	acoustic emission.
grp	glass fibre reinfored plastic.
cfrp	carbon fibre reinforced plastic.
F_c	fraction of a composite's volume represented by the CFP.
t_r	repeat thickness of laminate.
S_g	stiffness of GFP.
S_h	total stiffness of hybrid.
$\Delta\epsilon_t$	thermal strain mismatch.
ϵ_{ct}	thermally induced strain in CFP.

1. Introduction

Hybrid composites consist of two or more types of fibre in a common matrix. In recent years there has been a lively interest in such materials, particularly those which are based on a combination of glass fibre with one of the stiffer, but more expensive, carbon fibres. This interest stems from a belief that a more cost-effective utilization of the more expensive fibre may result if it is used in hybrid form. There is also some evidence that a hybrid structure will offer a more attractive combination of properties, e.g. stiffness and toughness, than composites based on a single fibre type. Summerscales and Short [1], have reviewed a number of studies of glass–carbon hybrid composites in which a phenomenon termed "synergistic strengthening" or the "hybrid effect" has been identified. This is defined in different ways by different workers, but the essential observation is that the failure strain, and hence the strength, of the low-elongation fibre (carbon) appears to be greater in a hybrid than in an all-carbon fibre composite structure.

The load bearing ability of a hybrid composite of uniaxially aligned fibres may be predicted from a diagram of the type shown in Fig. 1. The

0022–2461/81/082233–13$03.30/0

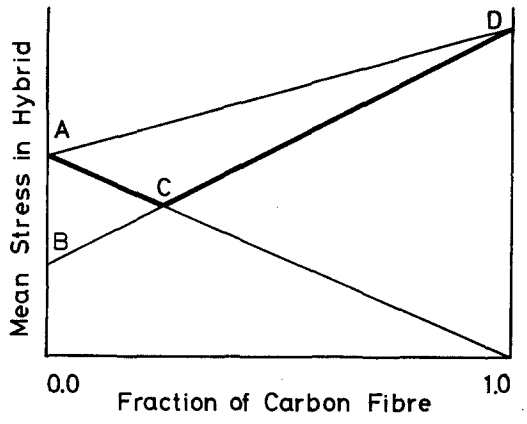

Figure 1 Theoretical strength of glass/carbon fibre hybrid composites. A and D are the strengths of the all-glass and all-carbon materials, respectively. BD is the stress in the hybrid at the failure strain of the carbon fibre.

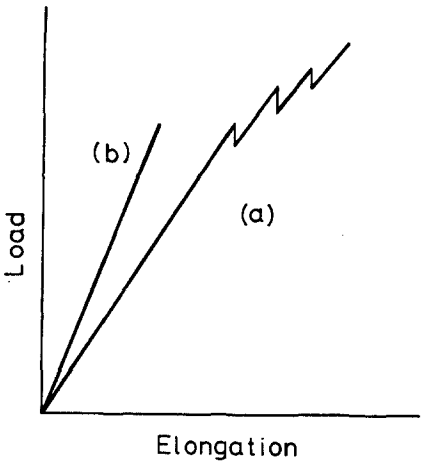

Figure 2 Schematic load–elongation curves showing, (a) multiple fracture and (b) single fracture.

horizontal axis depicts the fraction of carbon fibres in the structures which are all of identical total fibre content. The point A represents the tensile strength of the all-glass composite and D that of all-carbon composite. Since the carbon fibre has a lower elongation (0.01) than the glass (0.03), it may be expected that the first failure event will occur when the average strain in the composite exceeds the failure strain of the carbon failure. The line BD then represents the stress in the hybrid at which failure of the carbon fibre phase (CFP) will be expected. At low carbon fibre contents the glass fibre component (GFP) of the hybrid will be capable of carrying the extra load transferred to it by the failure of the carbon. The line AC is the ultimate strength of the hybrid in this condition. To the left of C the ultimate strength of the hybrid is determined by the glass, so that although the carbon will fail at BC the glass will continue to sustain the stress up to AC, when it too will fail. This is essentially the same argument as that advanced by Aveston and Kelly [2, 3] for multiple fracture of simple hybrid and non-hybrid composites. To the right of C the carbon will fail at CD and the glass will not sustain the load transferred and will, therefore, also fail. Load–elongation curves (displacement controlled loading) for these two conditions are shown in Fig. 2a and b. In Fig. 2a a failure in the CFP is marked by a load drop. On further extension the load continues to rise but there is a stiffness reduction due to transfer of load from the broken CFP to the GFP. Several failure events may occur in the CFP before final catastrophic failure of the GFP. In Fig. 2b the first CFP failure initiates a catastrophic failure sequence in the whole composite. Thus the line ACD in Fig. 1 marks the predicted ultimate strength of the hybrid and BCD the stress at first failure (of the carbon). Note that the simplistic rule-of-mixtures prediction, AD, is meaningless in this context. Now the hybrid effect may be defined as being any observations where the first failure stress lies above BCD or the ultimate stress above ACD. We express it as the percentage change (increase) of the failure strain of the carbon in the hybrid compared with that of an all-carbon composite.

Observation of the hybrid effect is first credited to Hayashi [4] and has subsequently been reported by several workers [5–11]. Some of their results are collected in Table I and the extent of the hybrid effect (HE) is indicated. Values ranging from 5 to 80% have been found. The effect may in part be explained by the fact that most of the composites tested were fabricated at elevated temperatures (to cure the resin), and subsequently cooled to ambient temperature. The carbon fibres were placed under compression due to the difference in thermal contraction between glass, resin and carbon. This is not however sufficient to explain the whole of the hybrid effect. The rest may be attributed to a size or dispersion effect. The results presented in Table II show the gross hybrid effect with no adjustment for the thermal contribution. Bunsell and Harris [7] report a large effect of 40 to 90%, but this is based on an uncommonly low value for the elongation of their carbon fibre, as noted by Aveston and Sillwood [8]. The latter sought to eliminate the thermal effect by selecting a room-temperature curing

TABLE I

Fibre types, lay-up sequence	Fibre volume fraction	Modulus (GPa)	Failure stress (GPa)	Failure strain	Fraction reinforced with low-elongation fibre	Hybrid effect, wrt low-elongation fibre (%)	Fabrication procedures, and other comments
Phillips [6]							
All glass	0.6	40	0.73	0.020	–	–	Unidirectional woven hybrid cloth with tows of glass and carbon alternating in the ratio given. Vinyl-ester matrix. Thermal strains not considered
All carbon	0.6	115	1.13	0.0098	–	–	
4 glass : 1 carbon	0.6	56	0.66	0.0118	0.2	20	
3 glass : 1 carbon	0.6	60	0.69	0.0115	0.25	17	
2 glass : 1 carbon	0.6	65	0.72	0.0111	0.33	13	
1 glass : 1 carbon	0.6	75	0.75	0.0100	0.5	2	
Bunsell and Harris [7]							
All carbon	0.6	142	0.40	0.0026	–	–	All hybrids laminated from preimpregnated fibre material Epoxy matrix
All glass	0.4	41	0.52	0.0125	–	–	
(1 glass, 2 carbon, 1 glass)	0.5	89	0.30	0.0037	0.5	42	
(1 glass, 1 carbon, 1 glass)	0.47	72	0.34	0.0048	0.33	85	Multiple fracture failure mode, with delamination, between plies of 3-layered sandwich
Aveston and Sillwood [8]							
All glass	–	–	–	–	–		Veil is 10^4 filament tow spread to 300 mm width, and combined with 204 filament glass tow in RT curing epoxy
Type I carbon "veil"	–	–	–	0.0050	–		
Carbon veil/glass tows	–	–	–	0.0108	0.1	116	
Marom et al. [9]							
All E-glass	0.5	25	0.70	0.028	–	–	Thermal contraction differences not considered
All AS carbon	0.5	97	1.2	0.0123	–	–	
(1 E-glass, 1 AS)n	0.5	61	0.85	0.0139	0.5	13	
(2 E-glass, 2 AS)n	0.5	61	0.83	0.0136	0.5	11	Epoxy resin matrix. Parameter n in lay-up sequence not specified
(5 E-glass, 5 AS)n	0.5	62	0.80	0.0129	0.5	5	
Zweben [10]							
All Kevlar	–	–	–	0.0180	–	–	Thornel 300 and Kevlar 49, alternating yarns in preimpregnated fibre material tapes. Differential thermal contractions not significant
All carbon	–	–	–	0.0104	–	–	
Kevlar/carbon tows	–	–	–	0.0108	0.5	4	

resin. Their hybrid contained highly dispersed carbon fibres and they reported elongation enhancements of up to 100%; however, their failure criterion was based on multiple failures of the carbon fibres and is not directly comparable with that adopted by other workers. Zweben [10] studied a Kevlar 49 – carbon fibre system in which tensile residual strains would be expected, leading to a negative hybrid effect. However he observed a small positive elongation enhancement (5%). The other workers quoted in Table I all obtained positive hybrid effects of an extent comparable to our own. To summarize: in all cases there is an enhancement of elongation of the carbon fibre phase. Where thermal strains have been considered they are too small, or of the opposite sense, to account for the whole of the observed effect. Where hybrids have been fabricated with a constant glass:carbon ratio (and therefore similar thermal effect), but with different degrees of dispersion, the hybrid effect is greater in the more highly dispersed materials. The aim of the present work has been to establish the role of glass:carbon ratio and the level of

TABLE II

Number of glass laminae	Number of carbon laminae	Number of glass laminae	Dispersion ($\times 10^{-3}\,m^{-1}$)	Carbon fraction	Modulus (GPa)	First-failure stress (GPa)	First-failure strain	Debond length (mm)	Hybrid effect/ size effect (%)	Thermal strain ($\times 10^{-3}$)
E-glass laminates										
3	0	0	2.67	0.00	45	1.20	0.0270	–	0.0	0.00
12	0	0	0.67	0.00	44	1.21	0.0280	–	0.0	0.00
HTS carbon/E-glass hybrid laminates										
0	1	0	8.00	1.00	126	0.97	0.0077	–	−33.0	0.00
0	2	0	4.00	1.00	128	1.13	0.0088	–	−24.0	0.00
0	3	0	2.67	1.00	143	1.48	0.0103	–	−10.0	0.00
0	4	0	2.00	1.00	129	1.25	0.0097	–	−16.0	0.00
0	12	0	0.67	1.00	144	1.66	0.0115	–	0.0	0.00
1	1	1	2.67	0.33	83	1.04	0.0125	32	8.7	0.39
2	1	2	1.60	0.20	65	0.92	0.0142	31	24.0	0.57
3	1	3	1.14	0.14	59	0.87	0.0148	17	29.0	0.67
4	1	4	0.89	0.11	60	0.90	0.0149	10	30.0	0.74
6	1	6	0.62	0.08	55	0.82	0.0150	6	30.0	0.82
9	1	9	0.42	0.05	49	0.76	0.0155	3	35.0	0.88
2	2	2	1.33	0.33	76	1.03	0.0135	> 100	17.0	0.40
3	2	3	1.00	0.25	72	0.97	0.0135	> 100	17.0	0.50
1	3	1	1.60	0.60	104	1.43	0.0137	100	19.0	0.18
3	3	3	0.89	0.33	77	1.04	0.0136	> 100	18.0	0.40
8	3	8	0.42	0.16	58	0.82	0.0141	> 100	23.0	0.64
3	8	3	0.57	0.57	102	1.38	0.0136	> 100	18.0	0.19
1	9	1	0.73	0.82	109	1.40	0.0129	> 100	12.0	0.07
8	9	8	0.32	0.36	81	1.03	0.0127	> 100	10.0	0.36
(1	1)	× 6	4.00	0.50	93	1.20	0.0129	–	12.0	0.24
(2	2)	× 3	2.00	0.50	90	1.23	0.0136	–	18.0	0.24

TABLE II (*continued*)

Number of glass laminae	Number of carbon laminae	Number of glass laminae	Dispersion ($\times 10^{-3}\,m^{-1}$)	Carbon fraction	Modulus (GPa)	First-failure stress (GPa)	First-failure strain	Debond length (mm)	Hybrid effect/ size effect (%)	Thermal strain ($\times 10^{-3}$)
HMS carbon/E-glass hybrid laminates										
0	3	0	2.67	1.00	184	1.11	0.0060	–	– 13.0	0.00
0	12	0	0.67	1.00	192	1.33	0.0069	–	0.0	0.00
1	1	1	2.67	0.33	95	0.75	0.0079	–	15.0	0.29
2	2	2	1.33	0.33	99	0.83	0.0084	–	22.0	0.29
3	3	3	0.89	0.33	89	0.75	0.0084	–	22.0	0.29
6	7	6	0.42	0.37	100	0.82	0.0082	–	19.0	0.26
8	3	8	0.42	0.16	65	0.55	0.0084	–	22.0	0.50
9	1	9	0.42	0.05	50	0.51	0.0101	–	46.0	0.73
(1	1)	× 4	4.00	0.50	119	0.95	0.0080	–	16.0	0.17
(2	2)	× 2	2.00	0.50	119	0.87	0.0073	–	6.0	0.17
Wet lay up composites										
All-carbon, all-glass										
All HTS carbon				1.00	135	1.52	0.0112	–	0.00	0.00
All E-glass				0.00	39	1.20	0.0300	–	0.00	0.00
HTS carbon divided-tow hybrids										
10 000 fibres				0.06	44	0.67	0.0150	14.30	30.00	1.41
3 620 fibres				0.02	41	0.66	0.0160	3.30	39.00	1.46
1 620 fibres				0.01	40	0.66	0.0165	0.71	43.00	1.48
630 fibres				0.004	39	0.69	0.0175	0.25	52.00	1.49

dispersion in determining the extent of the hybrid effect.

2. Experimental procedure

A range of unidirectional fibre hybrid laminates was made incorporating E-glass (G) with either high modulus (HMS) or high tensile strength (HTS) carbon fibres. Three distinct series of test laminates were fabricated and these are designed "alternating laminate" (AL), "divided tow" (DT) and "spread tow" (ST). The AL series was fabricated by hot-press moulding unidirectional preimpregnated fibre laminae of E-glass or carbon fibres in a proprietory epoxy resin (Fothergill and Harvey, Code 69). This system yielded laminates of approximately 0.6 fibre volume fraction, and the desired hybrid configuration was obtained by stacking the appropriate number of preimpregnated fibre sheets to form each lamina. One layer of preimpregnated fibre material was cured to give a lamina approximately 0.13 mm thick and within this restriction a range of laminates was made with varying carbon fraction, F_c, and dispersion. Most of these laminates were of a simple glass–carbon–glass sandwich form, but some multiple-layer laminates were also made. Details of all the laminates produced are given in Table II. It should be noted that since the basic unit of these laminae is a single layer of preimpregnated fibre material this limits the possible range and interval of both F_c and dispersion. Dispersion is defined as the reciprocal of the smallest repeat unit of the laminate as indicated in Fig. 3. Thus, a higher dispersion means that the constituents are in a more finely divided form.

Coupon test pieces, Fig. 4, made from the AL laminates were tested in tension, and the load and strain-at-failure of the central carbon lamina were measured. An acoustic emission monitoring system provided valuable information on the progress of failure in the material.

From the results of these tests it became apparent that it would be necessary to fabricate and test hybrids with a higher dispersion than was possible using the preimpregnated fibre system. The DT series were fabricated by a wet lay-up process, using an anhydride-cured bisphenol-based epoxy resin. The glass fibres were wound onto frames to form the outer glass reinforced layers and single bundles of carbon fibre were laid at intervals across the width of the laminate sheet (~ 20 mm intervals across 100 mm) so that ultimately each test coupon would contain just one bundle of carbon fibres running down the middle of the section, as shown in Fig. 4b. This bundle was either the full 10 000 filament tow, or a portion of it down to approximately 600 fibres. In the ST series a similar approach was employed but a very thinly spread-out tow was sandwiched between the glass reinforced layers, as shown in Fig. 4c. This was accomplished with the aid of a specially constructed tow-spreading device. The 10 000 filament tow was drawn through a divergent hydraulic nozzle whose action spread the tow into a thin veil some 35 mm wide. This was collected on a cotton gauze belt, dried, and subsequently cut to the required lengths for the laminates. This produced a thin, but rather variable, central lamina containing a range of fibre bundles ranging from single fibres to about 100, and averaging about 2 fibres thick (i.e. ~ 20 μm). Full details of the DT laminates are also given in Table II.

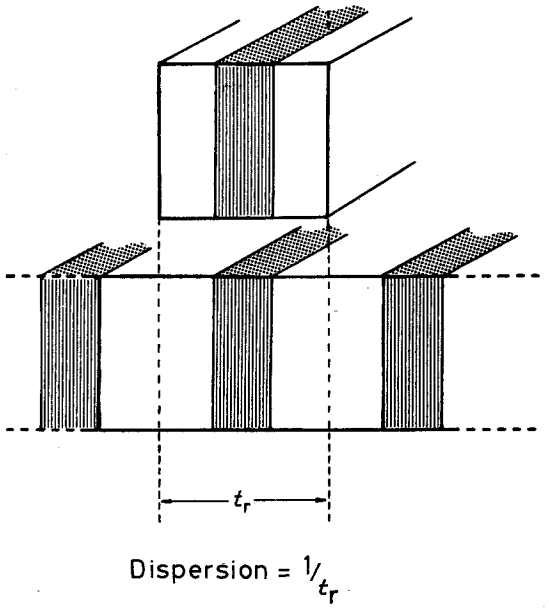

Figure 3 Definition of dispersion in sandwich and multiple-layer laminates.

Both the preimpregnated fibre, AL, and the wet lay-up laminates, DT and ST, were hot cured. The former to a maximum temperature of 175° C and the latter to 150° C. These temperatures are significant in determining the extent of the thermal strains in the material on cooling back to ambient temperature.

2.1. Laminated hybrids

The detailed results from the tensile tests on the

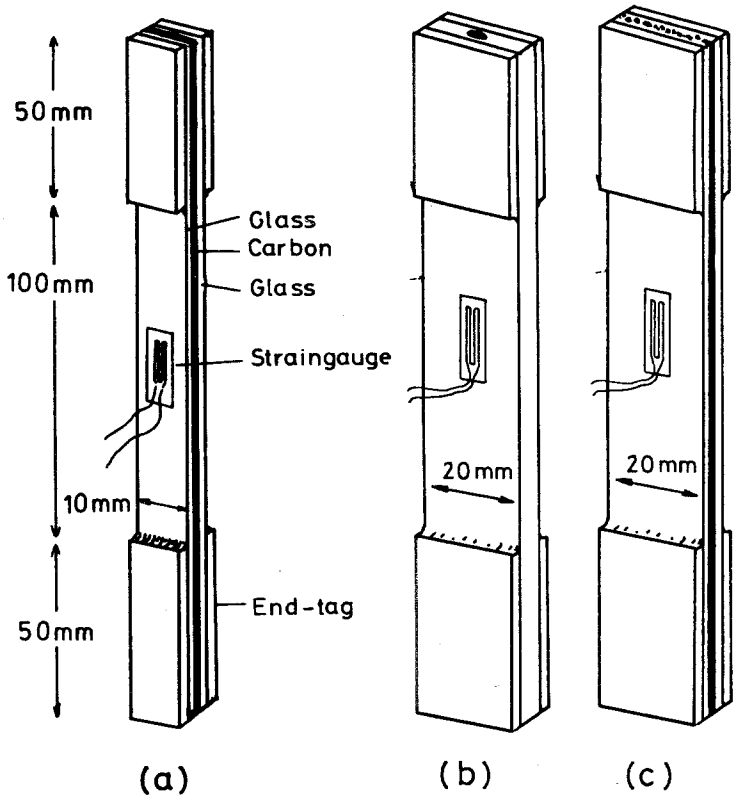

Figure 4 Test piece configurations (a) sandwich laminate (AL), (b) divided-tow (DT) and (c) spread-tow (ST).

laminated hybrids, AL series, and on all-glass and all-carbon (G, HTS and HMS series) laminates are given in Table II. Each entry is an average value calculated from five or more individual tests.

The G series comprised laminates of two thicknesses, (3 and 12 plies, respectively), which gave similar values for modulus, strength and failure strain. Failure initiated by longitudinal splitting which progressed to total disintegration of the test piece at final failure. This is typical of unidirectional glass fibre composites.

In contrast to the behaviour of the all-glass laminates the all-carbon (HTS and HMS) series failed by the propagation of a single transverse crack, with only limited longitudinal splitting. This difference in behaviour is considered to be attributable to the lower interfacial bond strength and also the much higher failure strain in the glass–epoxy system. Both the HTS and HMS series comprised laminates of several different thicknesses which were observed to fail at distinctly different strains. In both cases the thicker laminates failed at higher strains; about 20% higher for each doubling of laminate thickness up to 12 plies. This effect is not understood. It is in conflict with the trends observed in the same materials in hybrid form (AL series) and we are able to attribute it only to the imperfect fibre alignment in the preimpregnated fibre sheets, which appears to have had a more deleterious effect in the thinner laminates [12]. This trend is particularly unfortunate in the present context since it is necessary to use the properties of the all-carbon laminates as a control from which to establish the extent of any hybrid effect. We have chosen to use the thickest (12-ply) laminates as the standard because their properties were more consistent, and, since they failed at the highest strains, would give the lowest hybrid effect.

In the case of the hybrid laminates we have based our calculation of the hybrid effect on the first failure of the carbon-ply. This failure strain was not constant, in either series, but was found to increase as the carbon-ply thickness and/or the carbon fraction were decreased, (Table II). The results for the HTS series are also shown in Fig. 5a and b. The total hybrid effect is indicated by the extent to which the experimental points fall above the line BD in Fig. 5a and above the horizontal line in Fig. 5b. We have determined the extent of the thermal residual strain (see the Appendix) and this is indicated by the dotted lines on the figures. It is apparent that this thermal effect accounts for only part of the overall hybrid effect.

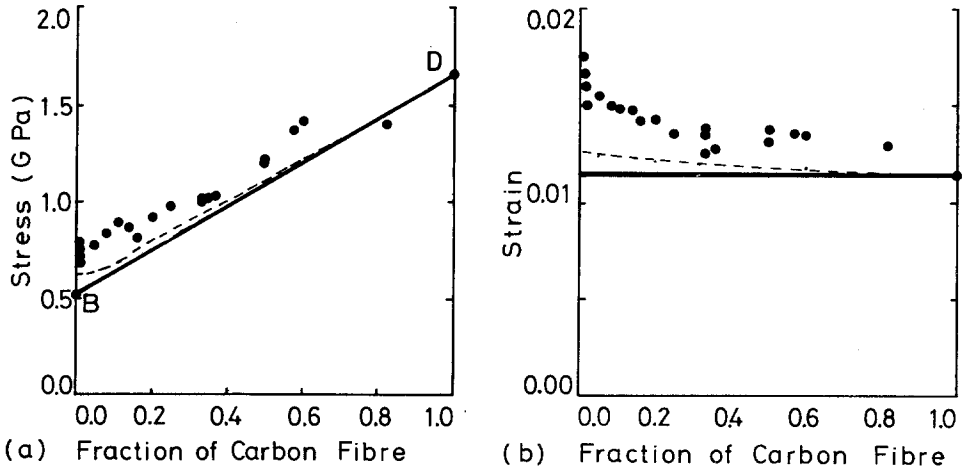

Figure 5 (a) Stress at first failure of the HTS carbon fibre phase in the AL series hybrid laminates. BD is drawn as in Fig. 1 and (b) strain at first failure of the carbon fibre phase in the AL and DT hybrid laminates. The broken lines indicate the expected point of failure when thermal effects are considered.

The load–strain curve was virtually linear up to the first-failure event and the modulus taken from this curve was found to be in agreement with the simple rule-of-mixtures prediction, as indicated in Table II. As the strain was increased the first macroscopic failure was a tensile fracture of the central carbon reinforced ply. This is shown schematically in Fig. 6; the principal transverse crack runs across the whole width and thickness of the carbon-ply. A delamination crack is produced at the intersection of the transverse crack with the outer glass plies. The extent of delamination varies according to the specimen geometry, and is greater when the carbon-ply is thicker and/or the glass-plies are thinner [12, 13]. In some cases the delamination extended over the whole length of the specimen, so that the carbon-ply became totally unloaded and final failure consisted merely of failure of the glass outer plies. When the delamination was less than the specimen gauge length, further extension after the initial failure event caused only limited growth of the delamination and further carbon-ply fractures occurred at random positions in the un-delaminated portions of the gauge length. The length of the delamination at each of these multiple fractures was found to be characteristic of a particular geometry, as shown in Table II.

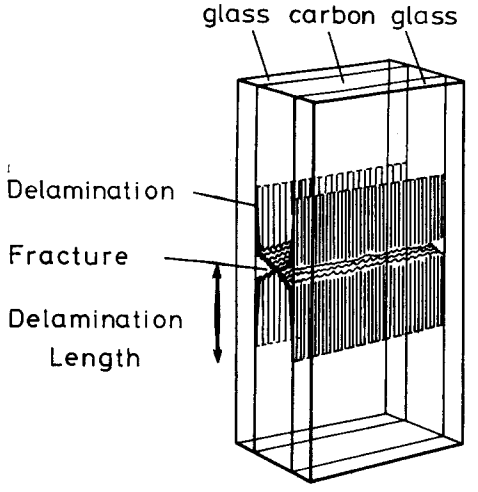

Figure 6 Failure mode of carbon-ply in AL series laminate.

The tensile tests were conducted at a constant rate of extension, so that when the carbon-ply fractured and partially delaminated from the glass, load was transferred from the carbon to the glass. This resulted in a sudden reduction in the observed load (since the displacement remained momentarily constant). The actual recorded form of the load–strain curve was dependent on the position of the strain gauge with respect to the delaminated zone(s). Fig. 7a and b show the load–strain curves for laminates with thick and thin carbon-plies, respectively. In the former the extent of the load drop was greater resulting in a characteristically jagged trace, whilst the latter was much smoother. In both cases, as the extension was increased, most of the gauge length became delaminated so that the stiffness and strength approached those of the glass-plies alone.

The practical significance of these observations is that the carbon-ply fracture does not propagate directly into the glass, but is diverted by the delamination cracks and, since these are of finite

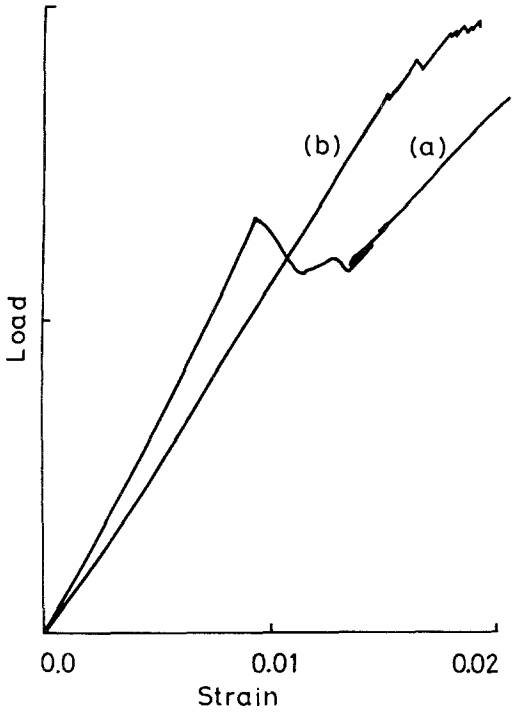

Figure 7 Experimental load–extension plots for typical AL series laminates (a) 0.38 mm carbon-ply, 1.02 mm glass-plies and (b) 0.13 mm carbon-ply, 1.14 mm glass-plies.

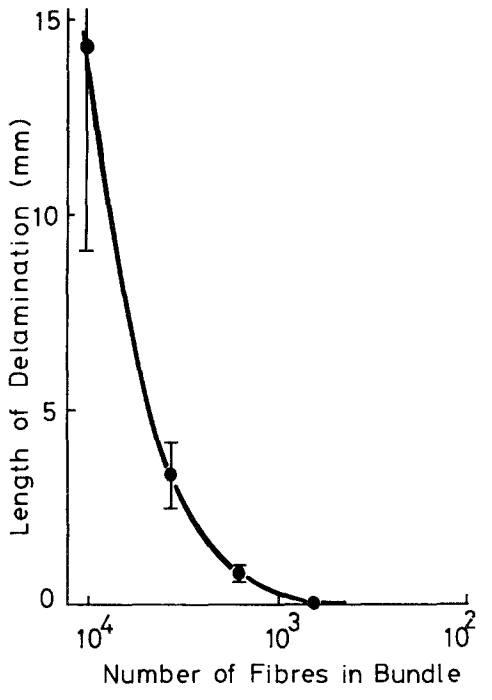

Figure 8 Delamination length against bundle size in DT series laminates.

length, it is clear that load must be diffused back into the carbon-ply across the delamination interface. This load transfer pattern has been confirmed by a study utilizing a laser-moiré strain visualization technique [13], and is an essential feature of the progressive multiple-cracking failure mode observed.

2.2. Divided-tow hybrids

The failure mode in the DT series was essentially similar to the multiple cracking observed in the AL series as shown in Fig. 6. Since the carbon fibre bundle amounted to only a small proportion of the cross-section, it had little influence on the overall stiffness of the test piece, and so individual fractures of the bundle caused negligible load drop. The delamination length was characteristic of the bundle size and was very much lower for smaller bundles, Fig. 8. Up to a strain of ~0.018 the number of cracks forming per unit length was greater for the larger bundles. Beyond this strain the crack density is higher for smaller bundles, as is shown by the curves in Fig. 9. This effect is surprising since a statistical theory of failure would imply that the rate should always increase with strain. However, we consider that the measured rate of crack formation is not directly related to the probability of failure, since the effective gauge length is reduced by the unloaded length (of the carbon) associated with each fracture. We assume that the carbon ligament is effectively unloaded over some characteristic distance, which is greater than the observed delamination length [13], either side of the fracture. There will, therefore, be little probability of another fracture occurring in this zone. We have taken the closest observed fracture spacing as an estimate of this length. (In fact we

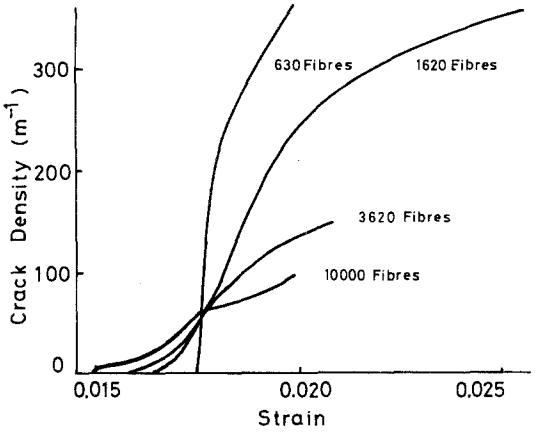

Figure 9 Crack density against strain in DT series laminates.

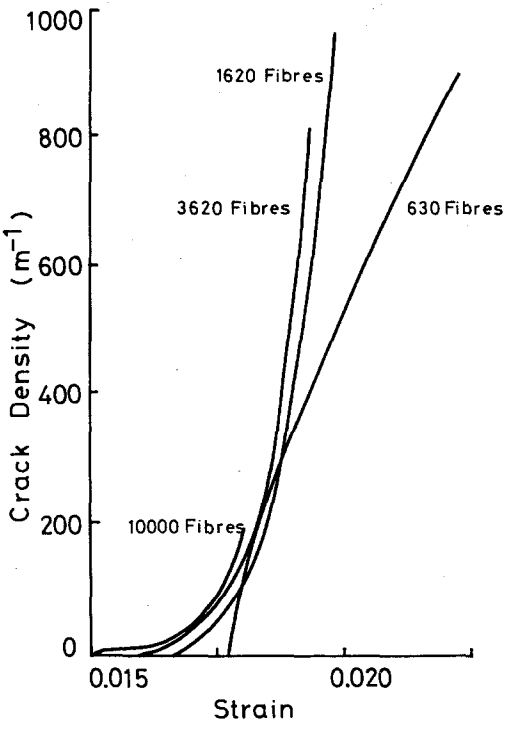

Figure 10 Crack density against strain curves for DT series adjusted for "unloaded length".

have averaged the 10% most closely spaced fractures.) The curves of Fig. 9 have been adjusted by multiplying the measured crack density by

$$[1 - (\text{measured crack density} \times \text{the unloaded length at each fracture})]$$

giving the curves shown in Fig. 10. This adjustment has relatively little effect when the cracks are widely spaced (i.e. at low strain) but becomes more significant as the crack spacing approaches the delamination length. All the curves in Fig. 10 are of a similar shape, but those for the smaller bundles are displaced to higher strains, showing hybrid effects of ~ 18 to 40% (based on first-failure of the bundle, and after allowing for residual thermal strains).

2.3. Spread-tow hybrids

When the spread tow hybrids were strained, isolated fibres and groups of fibres failed at random throughout the carbon reinforced layer, leading to a gradual accumulation of damage by multiple cracking of the carbon fibre bundles. Because the layer consisted of isolated bundles of carbon fibre separated by glass fibres, there was no single crack which propagated right across the layer, as was the case with the AL series. Fractures

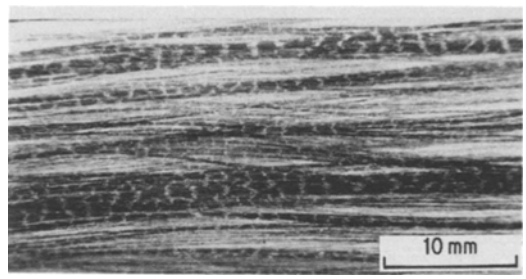

Figure 11 Optical photomicrograph showing multiple failure and debonding in ST series laminate.

in the larger bundles of fibres could be seen with the naked eye, Fig. 11, and were accompanied by delaminations similar to those in the DT series. Single carbon fibre fractures could be seen only under the microscope and are described in more detail in Part 2 [14] of this paper. The strain at which cracking first occurred could not be determined accurately because the damage was on such a fine scale, and it is doubtful whether the concept of a first-failure event is of value when there is a wide spectrum of bundle sizes. Acoustic emission monitoring gave a more useful general indication of the extent of microscopic damage.

2.4. Acoustic emission results

During straining microscopic damage accumulated by a number of mechanisms before any indication of macroscopic fracture. Acoustic emission (AE) monitoring was able to distinguish between noise sources associated with the fibre and associated with the resin. Although direct identification of these was not possible, there is substantial evidence that carbon fibre fractures and resin cracking are the major noise sources.

Acoustic emission curves for all the wet lay up composites are presented on a common strain axis in Fig. 12. The level of AE from the all-carbon composite, Fig. 12a, was very much greater than from the all-glass fibre composite, Fig. 12b, and is associated solely with the difference in fibre type as all other factors are the same, suggesting that fibre fracture is a major source. The AE rate from specimens of identical construction was consistent to within ± 20% (at equal strains), whereas the difference between glass and carbon composites is a factor of about 60 at 0.01 strain.

Up to first failure of the carbon bundle at the peak of the AE curves, all the divided-tow hybrids showed a similar pattern of emission, Fig. 12c to f, following closely that from the all-carbon com-

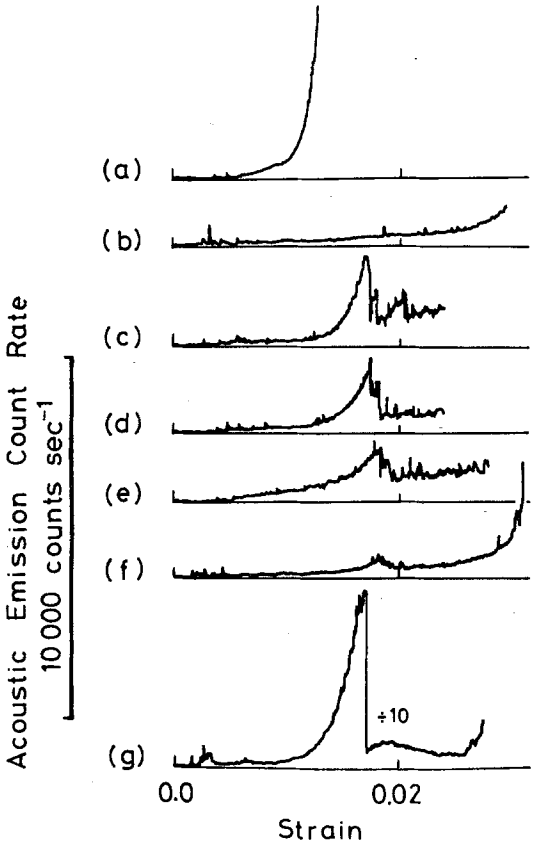

Figure 12 Acoustic e (d) 3600 filament bundle; (e) curves for wet lay up DT 1600 filament bundle, (f) 620 laminates (a) all-carbon, filament bundle and (g) ST glass, (c) 10 000 filament laminate.

posite but at a lower level. During multiple cracking the AE rate was lower and more irregular than just before the first failure, but the AE rate rose again to a second maximum at ultimate failure, following the high strain behaviour of the all-glass AE curves. At these high strains the carbon bundle is extensively fractured and decoupled from the glass plies by delamination, so the total acoustic emission appears to be simply the sum of emissions from glass and carbon reinforced components.

Acoustic emission rate curves for the spread-tow hybrids have no sharp peak at the onset of multiple cracking, but have instead a broad hump centred around 0.019 strain, Fig. 12g. The AE rate then falls by about half before rising again to a maximum at failure (~ 0.03 strain), reflecting the underlying behaviour of the glass-plies. Glass-ply thickness makes little difference to the level of emission in these laminates, so there can be little attenuation through such a thickness of GFP.

Optical micrographs of the all-glass fibre wet

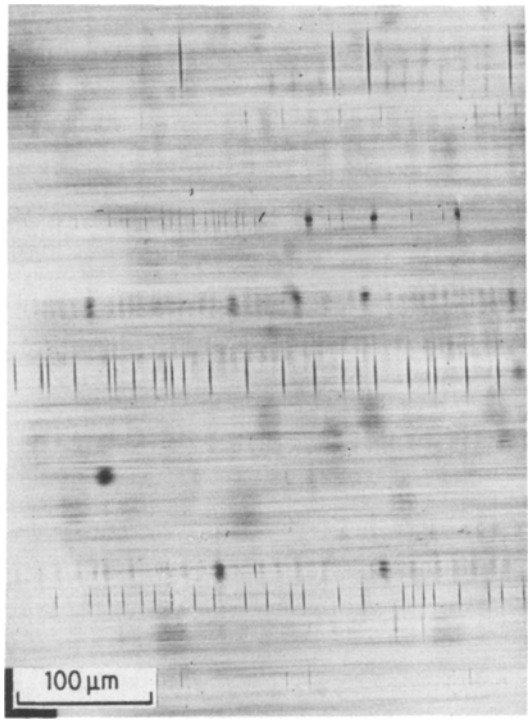

Figure 13 Optical photomicrograph showing matrix cracks in all-glass laminate strained to 0.023.

lay-up specimens taken in transmitted light show extensive matrix cracking above 0.02 strain, Fig. 13, and the number of these cracks correlates well with the total number of emissions, suggesting that this is a major source, Fig. 14. Glass fibre fractures have not been observed in this way. There was little difference in AE between laminated hybrids

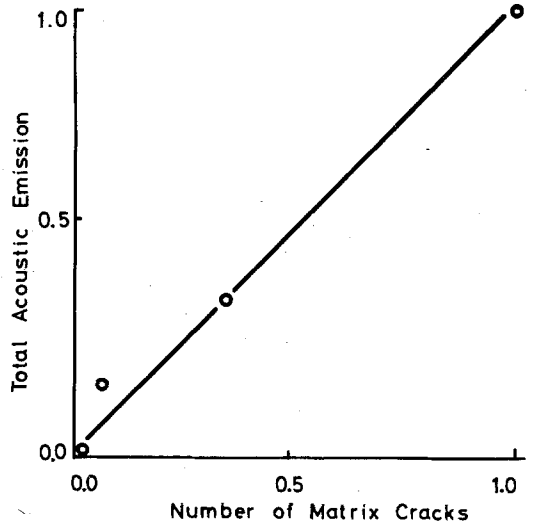

Figure 14 Correlation between acoustic emission and number of matrix cracks for all-glass laminate.

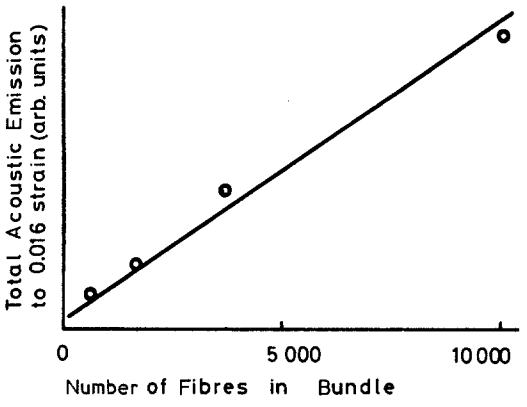

Figure 15 Correlation between acoustic emission and bundle size for DT laminates.

of different geometries, and the much higher level suggests that sources associated with the carbon fibres were masked by emissions from the lower elongation Code 69 resin.

The AE total from the divided-tow hybrids, (integrated to 0.016 strain), is proportional to the number of fibres in the bundle, Fig. 15. (The contribution from the GFP is insignificant here), and this is further evidence that fibre fracture is the major AE source.

3. Conclusions

The results of this work have clearly confirmed the existence of the hybrid effect. Its extent is dependent on the ratio of the two fibre types and upon their dispersion. In general a higher failure strain is observed in the less extensible, stiffer fibre when it is more finely dispersed and occupies a lower proportion of the volume. This is in agreement with other published work [5–11].

The hybrid strain enhancement effect is in part due to the thermal strains induced in the material, but the extent of these strains is sufficient to account for only a small proportion of the observed effect.

In grp laminates containing less than a critical volume of dispersed cfrp a progressive failure mode is observed. The cfrp component fails in an essentially brittle manner with debonding between cfrp and grp components.

The extent of this debonding or delamination is critically dependent on the size of the cfrp unit (bundle diameter or lamina thickness) and in favourable cases a multiple cracking mode is developed. In such hybrids the initial stiffness is enhanced in proportion to the cfrp content but the brittle and catastrophic failure mode of the all-cfrp laminate is avoided. We conclude that properly engineered hybrids provide scope for limited improvements in the balance of stiffness and toughness in composite laminates.

In Part 2 [14] of this paper we account for the non-thermal part of the observed hybrid effect in terms of the relationships between strength and volume in brittle materials.

Comparison of AE rate curves for hybrid, all-carbon, and all-glass fibre composites, indicates that the failure of carbon fibres is a major source of emissions. However, in Part 2 [14] we show that the number of such fractures is relatively small in relation to the amount of fibre involved.

Acknowledgements

Carbon fibre for this work was kindly provided by Courtaulds Ltd. One of us (PWM) is grateful for financial support from contributions made by British Aircraft Corporation Ltd (now British Aerospace) to the University of Surrey appeal funds.

Appendix

Thermally induced strains

When hybrid composites are cooled after curing, residual strains are developed on account of the difference in thermal expansion coefficients between volumes reinforced with each type of fibre. These strains cannot be readily estimated from the cure temperature and expansion data because the effective solidification temperature will depend on the relaxation occurring in the resin. An additional complication is non-linearity of thermal expansion in cfrp and grp. For the laminated hybrids it was possible to measure residual strains directly from the bending in unbalanced laminates. This method was not suitable in the case of the wet lay up composites because the ply thickness could not be controlled with sufficient accuracy, and instead an upper bound for thermal strains was estimated from measurements of expansion coefficients.

Unbalanced laminates were moulded with 2 preimpregnated fibre materials each of E-glass and HTS or HMS carbon fibre, and were held flat during the post-cure and subsequent cooling to simulate conditions in a balanced laminate. The plates were cut into 5 strips each, and their curvatures were measured. The bending stiffness of each beam was determined by a 3-point bend test, and simple beam theory was used to derive the average

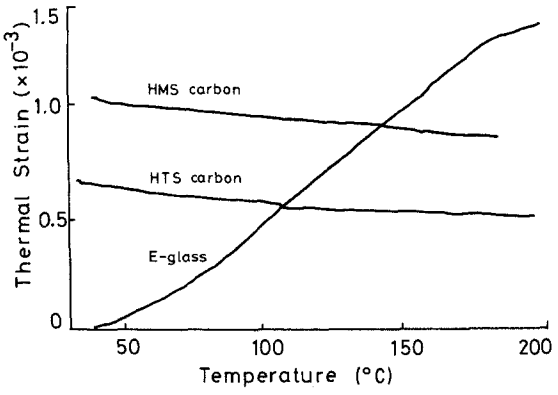

Figure A1 Thermal expansions in fibre direction of constituent phases of DT series.

stresses which would exist if the beam was constrained flat as it would be in a balanced construction. The thermal strain mismatch was

1.04×10^{-3} for HTS carbon/E-glass

and

0.93×10^{-3} for HMS carbon/E-glass.

The fraction of the strain mismatch ($\Delta\epsilon_t$) which appears as a compression of the carbon component in a balanced hybrid is given by the ratio of the stiffness of the GFP (S_g) to the stiffness of the hybrid as a whole (S_h). The carbon compression $\epsilon_{ct} = S_g \Delta\epsilon_t / S_h$ and that part of the hybrid effect which can be attributed to thermal strain is listed in Table II and indicated in Fig. 5.

Thermal expansions of the wet lay-up composites were measured in the fibre direction between 30 and 200° C with a Du Pont thermomechanical analyser, Fig. A1. Both HMS and HTS carbon composites were nearly linear, but the E-glass composite showed significant non-linearity near the limit temperatures. Best straight lines to these curves in the range 25 to 150° C give the following expansion coefficients:

HMS carbon – $1.00 \times 10^{-6} K^{-1}$;

HTS carbon – $0.91 \times 10^{-6} K^{-1}$;

E-glass – $10.60 \times 10^{-6} K^{-1}$.

The effective solidification temperature could not be measured, but it cannot exceed the post-cure temperature of 150° C, so in cooling to the test temperature of 20° C the maximum possible strain differential is 1.50×10^{-3} for HTS carbon and E-glass fibre. Virtually all this strain mismatch is accommodated by compression in the carbon fibre component since in all these composites the glass fibre contributes more than 94% of the total stiffness, making differences between geometries insignificant (ϵ_{ct} is 1.41×10^{-3} for 10 000 fibres, 1.46×10^{-3} for 3620 fibres, 1.48×10^{-3} for 1620 fibres and 1.49×10^{-3} for 630 fibres).

References

1. J. SUMMERSCALES and D. SHORT, *Composites* 9 (1978) 157.
2. J. AVESTON and A. KELLY, *Phil. Trans. Roy. Soc.* **A294** (1980) 519.
3. *Idem, J. Mater. Sci.* 8 (1973) 352.
4. T. HAYASHI *et al., Fukugo Zairyo (Composite Mater.)* **2** (1975) 18.
5. L. N. PHILLIPS, *Composites* 7 (1976) 7.
6. *Idem,* Proceedings of the International Conference on Composite Materials, Toronto, 1978 (AIME, New York, 1978).
7. A. R. BUNSELL and B. HARRIS, *Composites* **5** (1974) 157.
8. J. AVESTON and J. M. SILLWOOD, *J. Mater. Sci.* **11** (1976) 1877.
9. G. MAROM, S. FISCHER, F. R. TULER and H. D. WAGNER, *ibid.* **13** (1978) 1419.
10. C. ZWEBEN, *ibid* **12** (1977) 1325.
11. H. E. EDWARDS, N. J. PARRAT and K. D. POTTER, Proceedings of the International Conference on Composite Materials, Toronto, 1978 (AIME, New York, 1978).
12. P. W. MANDERS, PdD thesis, University of Surrey, 1979.
13. P. W. MANDERS and S. M. BISHOP, Investigation of Fracture in Hybrid Composites using a Laser Moire Technique, Royal Aircraft Establishment, Technical Memo. MAT 333, 1980.
14. P. W. MANDERS and M. G. BADER, *J. Mater. Sci.* **16** (1981) 2246.

Received 9 December 1980 and accepted 5 February 1981.